ACS SENSORS

pubs.acs.org/acssensors

Article

Engineering a Fluorescent Protein Color Switch Using Entropy-Driven β-Strand Exchange

Anna Miriam John, Harsimranjit Sekhon, Jeung-Hoi Ha, and Stewart N. Loh*

Cite This: *ACS Sens.* 2022, 7, 263−271

Read Online

ACCESS | Metrics & More | Article Recommendations | Supporting Information

ABSTRACT: Protein conformational switches are widely used in biosensing. They are often composed of an input domain (which binds a target ligand) fused to an output domain (which generates an optical readout). A central challenge in designing such switches is to develop mechanisms for coupling the input and output signals *via* conformational changes. Here, we create a biosensor in which binding-induced folding of the input domain drives a conformational shift in the output domain that results in a sixfold green-to-yellow ratiometric fluorescence change *in vitro* and a 35-fold intensiometric fluorescence increase in cultured cells. The input domain consists of circularly permuted FK506 binding protein (cpFKBP) that folds upon binding its target ligand (FK506 or rapamycin). cpFKBP folding induces the output domain, an engineered green fluorescent protein (GFP) variant, to replace one of its β-strands (containing T203 and specifying green fluorescence) with a duplicate β-strand (containing Y203 and specifying yellow fluorescence) in an intramolecular exchange reaction. This mechanism employs the loop-closure entropy principle, embodied by the folding of the partially disordered cpFKBP domain, to couple ligand binding to the GFP color shift. This study highlights the high-energy barriers present in GFP folding which cause β-strand exchange to be slow and are also likely responsible for the shift from the β-strand exchange mechanism *in vitro* to ligand-induced chromophore maturation in cells. The proof-of-concept design has the advantages of full genetic encodability and potential for modularity. The latter attribute is enabled by the natural coupling of binding and folding and circular permutation of the input domain, which theoretically allows different binding domains to be compatible for insertion into the GFP surface loop.

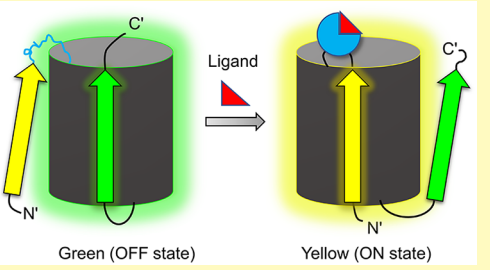

KEYWORDS: *alternate frame folding, fluorescent protein biosensor, loop entropy, protein conformational switch, protein engineering*

Protein switches are versatile tools with applications in synthetic biology, molecular diagnostics, and cellular biosensing.[1−4] Rapid advancements in the field of protein switch engineering using random, rational, semirational, and *de novo* approaches testify to the ongoing search for improved designs.[5−8] Many of these efforts aim to achieve two key goals: signal transduction (i.e., a strategy for joining recognition and reporter domains such that the signaling event is transduced to a detectable output) and modularity (the capability of substituting different recognition domains for sensing a target of choice).[9,10] In this study, we address these challenges by employing a combination of two protein engineering strategies—loop-closure entropy[11] and alternate frame folding (AFF[12])—to create a conformationally driven biosensor in which ligand binding and change in fluorescence color/intensity comprise the respective input and output signals.

AFF is a mechanism by which allostery is introduced into a protein which previously had none. AFF entails copying a terminal segment of a protein that contains a key functional residue, for example, one that binds a target ligand, essential to enzymatic function, or specifies light absorption/emission wavelengths, and pasting it to the opposite terminus of the parent protein. The presence of two identical segments allows the protein to switch between two folding "frames", one of which corresponds to the original amino acid sequence and the other to that of a circular permutant (CP). The two folds are mutually exclusive because the duplicated segments compete for the shared region. Changing the identity of the key residue in one of the segments links the fold shift to a change in protein function. We previously applied the AFF methodology to proteins that bind calcium (calbindin D_{9k}[12,13]) and a sugar (ribose-binding protein[14]) to convert them to biosensors for their respective ligands. Förster resonance energy transfer (FRET) output was achieved by attaching chemical fluorophores to sites that reported on the fold shift.

Here, we introduce two new features to the AFF design: full genetic encodability and a novel mechanism (loop-closure entropy) for transducing ligand binding to a fluorescence change. We demonstrate proof of concept by creating a genetically encodable protein switch that functions as a small-

Received: October 21, 2021
Accepted: December 28, 2021
Published: January 10, 2022

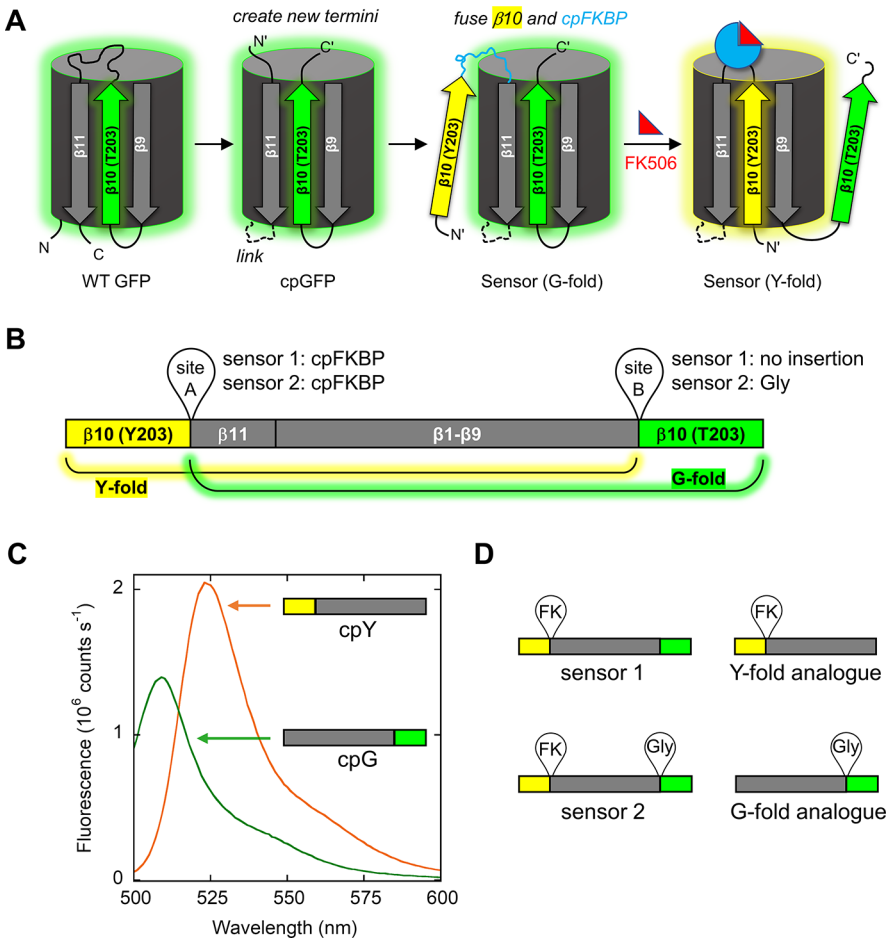

Figure 1. Design of esAFF sensors. (A) Sensors 1 and 2 were created by circularly permuting GFP at the loop between β10 (green, with T203) and β11 and joining the original termini with a six-amino acid linker (dashed loop). The new termini are designated N′ and C′. A duplicate β10 strand (yellow, with Y203) and cpFKBP (blue) were then appended to N′, establishing the mutually exclusive G-fold and Y-fold. The gray β-strands and cylinder represent the structure shared between the G-fold and Y-fold. In the absence of the ligand, the cpFKBP domain is mostly disordered, and the sensor populates the G-fold. Upon binding FK506 or rapamycin, the cpFKBP domain becomes structured and stabilizes the Y-fold. (B) Linear depiction of the esAFF switch showing the locations in which the receptor domain (site A) and thermodynamic tuning peptides (site B) were inserted to generate sensor 1 and sensor 2. Color schemes are identical to those in panel (A). (C) Superimposing fluorescence spectra of the isolated green (cpG, green trace) and yellow (cpY, orange trace) switch components, recorded at the same protein concentration and excitation wavelength (492 nm), illustrating the maximum theoretical sensor response from fully green to fully yellow. cpY is 1.675 times brighter than cpG, as defined by the integrated AUCs. cpY and cpG, depicted schematically in the inset, lack any insertion at site A or site B. (D) Cartoon representations of the constructs created for this study are shown with color coding, as in panel (B).

molecule-induced ratiometric biosensor *in vitro* and an intensiometric biosensor in mammalian cells. This biosensor is designed to be generalizable by inserting different recognition domains into the same fluorescent protein (FP) scaffold.

EXPERIMENTAL SECTION

Gene Construction and Protein Purification. Amino acid sequences for all protein constructs are shown in Figure S12. Genes were cloned in a pET41b plasmid vector and fully sequenced. Proteins were expressed in *Escherichia coli* BL21 (DE3), with isopropyl β-D-thiogalactopyranoside induction occurring at 18 °C for 16−18 h. Cell pellets were resuspended in 20 mM Tris (pH 8.0), 300 mM NaCl, 10 mM imidazole, and 10 mM β-mercaptoethanol and lysed using a small amount of hen lysozyme, followed by sonication. The soluble fraction was loaded onto a nickel nitrilotriacetic acid column (Bio-Rad, Hercules, CA), and proteins were purified following the manufacturer's protocols. Eluted proteins were dialyzed into buffer containing 10 mM Tris (pH 7.5) and 150 mM NaCl. Each sensor construct was eluted as a monomeric species from a Superdex S200 Increase size exclusion column (Cytiva) and was judged to be >95% pure by SDS-PAGE (Figure S5). The circularly permuted FKBP gene was inserted into the *Thermoanaerobacter tengcongensis* ribose-binding protein gene, as described by Ha *et al.*[15] The cpFKBP−RBP fusion protein was expressed and purified as described above, after which RBP was cleaved off using HRV-3C protease. Free circularly permuted FK506 binding protein (cpFKBP) was recovered by passing the digested solution through a nickel− nitriloacetic acid column to remove free RBP and undigested cpFKBP−RBP.

Spectroscopic Measurements. Fluorescence spectra were recorded on a Horiba Jobin Yvon Fluoromax-4 benchtop fluorometer or a Molecular Devices Spectramax i3x plate reader. Settings for the benchtop fluorometer were 492 nm excitation (2 nm bandpass) and 500−600 nm emission (3 nm bandpass). Settings for the plate reader were 470 nm excitation and 500−600 nm emission. Refolding kinetics of cpFKBP was monitored by excitation at 280 nm (2 nm bandpass) and emission at 355 nm (6 nm bandpass).

Protein Stability Determination. Solutions for denaturation experiments were prepared by mixing a solution of 20 mM Tris pH 8.0, 150 mM NaCl, 1 mM TCEP, and 0.1−0.5 μM FP (or 3 μM cpFKBP) with an identical solution containing 1.0−4.4 M GdmCl,

https://doi.org/10.1021/acssensors.1c02239
ACS Sens. 2022, 7, 263−271

using a Hamilton Microlab 540B dispenser. Final denaturant concentrations were measured from the refractive index. Samples were incubated for 24 h at 37 °C (FPs) or 8 h at room temperature (cpFKBP). Green/yellow fluorescence spectra of FP samples were recorded on the plate reader, and cpFKBP Trp emission data were collected on the benchtop fluorometer. GdmCl denaturation curves were fit to the linear extrapolation equation[16] to obtain ΔG and m values.

Spectral Unmixing. Fluorescence spectra were unmixed by fitting the data to eq 1 using MATLAB's built-in nonlinear regression function (nlinfit)

$$\text{signal}_{\text{tot}} = \chi_{\text{green}} \times \text{ref}_{\text{green}} + \chi_{\text{yellow}} \times \text{ref}_{\text{yellow}} \quad (1)$$

where $\text{signal}_{\text{tot}}$ is a 100-element vector consisting of the raw signal at each wavelength (500−600 nm); $\text{ref}_{\text{green}}$ and $\text{ref}_{\text{yellow}}$ are the signals from the reference cpG and cpY spectra; and χ_{green} and χ_{yellow} are scalars that correspond to the relative contributions of the green-fold (G-fold) and yellow-fold (Y-fold). $\text{AUC}_{\text{green}}$ and $\text{AUC}_{\text{yellow}}$ were calculated by integrating $\chi_{\text{green}} \times \text{ref}_{\text{green}}$ and $\chi_{\text{yellow}} \times \text{ref}_{\text{yellow}}$, respectively.

Fluorescence microscopy images were unmixed in a similar way, except that $\text{signal}_{\text{tot}}$, $\text{ref}_{\text{green}}$, and $\text{ref}_{\text{yellow}}$ were vectors consisting of only two elements [the total signal from each pixel, the total signal of the G-fold, and the total signal of the Y-fold, in the green (excitation 470/40 and emission 525/50) and yellow (excitation 500/20 and emission 530/50) channels]. We verified this method by mixing various ratios of purified G-fold and Y-fold analogues, imaging the solutions under the fluorescence microscope, and finding that the method accurately predicted their relative contributions.

***In Vitro* Switching Experiments.** Sensors were unfolded at room temperature by adding two-thirds volume of 50 mM HCl. After 2 min, the proteins were refolded by 1/30 dilution into experimental buffer [25 mM Tris (pH 7.5), 150 mM NaCl, 0.1 mM EDTA, and 1 mM TCEP]. The final protein concentration was ∼0.2 μM. The proteins were allowed to refold until all spectral changes were complete (1 h at 45 °C), at which point either 20 μM FK506 (ON state) or vehicle (0.04% DMSO; OFF state) was added. The fluorescence spectra were recorded on the Fluoromax-4 fluorometer, as described above. The turn-on values were calculated by dividing $(\text{Y/G})_{\text{ON}}$ by $(\text{Y/G})_{\text{OFF}}$ at the indicated time points.

To evaluate the possible contribution of a dark-to-yellow process to the observed turn-on, we first calculated the loss in the concentration of G-fold after FK506 addition by $\text{AUC}_{\text{green,OFF}} - \text{AUC}_{\text{green,ON}}$. If the increase in yellow fluorescence was due exclusively to the AFF-mediated fold shift, then the theoretical change in Y-fold concentration is equal to $(\text{AUC}_{\text{green,OFF}} - \text{AUC}_{\text{green,ON}}) \times 1.675$ (the factor by which cpY is brighter than cpG; Figure 1C). In this ideal condition, the observed value of $\text{AUC}_{\text{yellow,ON}}$ would be $\text{AUC}_{\text{yellow,OFF}} + (\text{AUC}_{\text{green,OFF}} - \text{AUC}_{\text{green,ON}}) \times 1.675$. The percentage of turn-on due to the AFF mechanism is reported as $[(\text{AUC}_{\text{green,OFF}} - \text{AUC}_{\text{green,ON}}) \times 1.675 \times 100]/(\text{AUC}_{\text{yellow,ON}} - \text{AUC}_{\text{yellow,OFF}})$. For *in vitro* experiments, these values were 100% within experimental error, indicating that no dark-to-yellow component was present.

COS-7 Cell Culture and Imaging. The sensor 2 gene was transiently transfected under the constitutive CMV promoter and expressed for 36−48 h before adding rapamycin or DMSO vehicle in serum-free media. Turn-on was quantified by dividing the average intensity of each cell in the unmixed yellow channel by the average intensity in the unmixed green channel (Y/G). COS-7 cells were maintained in Dulbecco's modified Eagle medium (DMEM) with 10% FBS and pen/strep antibiotics in an incubator with 5% CO_2 at 37 °C. The cells were split into fresh media 1 day before transfection in a six-well plate, so that they reached 60−80% confluency the next day. The freshly prepared miniprep DNA (1.5 μg of pCMV-mKate2-N and 1.5 μg of pCMV-MBP-sensor 2 or 1.5 μg pCMV-MBP-Y-fold analogue) was then transfected using the calcium phosphate method,[17] with the following modifications. $CaCl_2$ was added to the plasmid mix to the final concentration of 250 mM (150 μL final volume), and 150 μL of 50 mM HEPES, 1.5 mM sodium phosphate (pH 7.0), and 150 mM NaCl was then added dropwise while vortexing. The transfection mixture was added directly to the media after aging at room temperature for 15 min, and the media was changed 12−15 h after transfection. 36−48 h after transfection, the cells were washed with imaging media (DMEM, 25 mM HEPES, pH 7.0, with no FBS), and either rapamycin or the DMSO vehicle was added to the cells diluted into the imaging media. The cells were treated with 5 μM rapamycin for 4 h to quantify the maximum turn-on and for time points ranging from 30 min to 4 h to determine the turn-on rate.

The cells were mounted in imaging media and imaged with a Zeiss Axioimager Z1 upright microscope (40×/0.75 Plan-Neofluar objective) equipped with a mercury lamp, using the following filters: excitation 470/40, emission 525/50 for the green channel and excitation 500/20, emission 530/50 for the yellow channel. Cells were randomly picked using mKate2 fluorescence. At least 10 fields were imaged for each replicate. For technical repeats (≥2 per sample), the cells were split into a six-well dish on the same day and transfected from the same transfection mix, and for biological repeats (≥3 for each construct), the cells were transfected by a fresh miniprep plasmid DNA on different days.

All cell images were processed using Fiji.[18] Background was subtracted from each channel using the built-in plugin, and the acquired image was then compressed using the resize plugin from ImageJ to reduce the processing time. Each pixel of the resulting image was then unmixed to minimize the cross talk between the green and yellow channels using a custom MATLAB script, as described above. Briefly, purified G-fold analogue and Y-fold analogue were imaged using the same settings to determine the cross talk of each channel into the other, and this information was applied to linearly unmix the image of interest into their respective green and yellow contributions. Once unmixed, the intensity of each cell was measured in Fiji by manually drawing a region of interest around the periphery and determining the average intensity inside the region in both yellow and green channels. To quantify the turn-on for sensor 2, the yellow intensity for each cell was divided by the green intensity for that cell (Y/G), and for the Y-fold analogue, only the yellow channel was imaged and quantified. Green fluorescence was judged to originate from sensor 2 and not from background autofluorescence by the following criteria. First, untransfected cells in the same field were identified (by the lack of mKate2 fluorescence) and found to have no significant green (or yellow) autofluorescence. Second, cells transfected with the plasmid expressing the G-fold analogue exhibited 4.2-fold higher fluorescence ($p = 0.003$ by the unpaired t test) compared to the untransfected cells. The green fluorescence in the data analysis is therefore attributed to sensor 2 folding into the green frame.

RESULTS

Biosensor Design. The biosensor color change is made possible by switching between two amino acids at position 203 in the strand β10 of the 11-stranded β-barrel of a modified Clover GFP[19] (referred to as green fluorescent protein (GFP) in this paper). Residue 203 contacts the chromophore (G65−Y66−G67) that resides between β3 and β4. Replacing T203 with Y203 shifts the emission maximum from 509 nm (green) to 524 nm (yellow).[20,21] To enable the AFF conformational change, we employed the design introduced by Boxer and colleagues to construct a light-driven, fluorescent protease sensor.[22] GFP was first engineered to terminate its sequence with β10 instead of β11. This was achieved by circularly permuting it between β10 and β11 and joining the original N- and C-termini with a GGGSGG linker (Figure 1A). We then appended a duplicated β10, carrying the T203Y mutation, to the N-terminus of the CP to generate the FP scaffold (Figure 1B). The resulting fusion protein can adopt either the G-fold (GFP permuted between β10 and β11 and with T203) or the

https://doi.org/10.1021/acssensors.1c02239
ACS Sens. 2022, 7, 263−271

Table 1. *In Vitro* Characterization of esAFF Sensors[a]

sensor ([GdmCl])	turn-on	$t_{1/2}$ (h) Y-fold	$t_{1/2}$ (h) G-fold	% turn-on due to AFF
1	1.11	NA	NA	NA
2	5.97 ± 0.83	4.16 ± 1.1	5.76 ± 0.43	89.8 ± 15.5
2 (0.15 M)	6.64 ± 1.41	5.58 ± 2.06	5.52 ± 1.6	99.3 ± 8.9
2 (0.3 M)	6.32 ± 0.59	6.39 ± 1.40	5.73 ± 2.72	110 ± 5.5

[a]The values represent the average ± SD (n = duplicate or triplicate). esAFF and NA denote entropy-switching AFF and not applicable, respectively.

Y-fold (GFP permuted between β9 and β10 and with Y203). The conformational change consists of the duplicate β10 strands exchanging from the common core of β11 and β1−β9 (Figure 1A).

We linked the fold shift to molecular recognition using the principles of loop-closure entropy and binding-induced folding. Loop-closure entropy refers to the loss of chain entropy that results from constraining the termini of a disordered, flexible polypeptide to a single, fixed position.[11,23] If a protein contains a long, intrinsically disordered surface loop, the loop is free to adopt a normal distribution of end-to-end distances when the protein is unfolded, but its ends are constrained when the protein is folded. This unfavorable loss of chain entropy, theoretically proportional to the logarithm of the number of residues in the loop, is offset by the favorable free-energy change of protein folding. Deleting or shortening flexible surface loops is thus a common strategy for stabilizing proteins. Here, we take the opposite approach and insert a disordered recognition domain into a surface loop of a host protein. The entropic penalty paid by folding of the host goes away when the ends of the recognition domain become fixed by another process, for example, binding-induced folding. If the distance between the termini of the folded recognition domain is compatible with the structure of the host protein at the insertion point, the host becomes stabilized by ligand binding.

To drive the color change of the FP scaffold in Figure 1B, one can insert the disordered recognition domain (cpFKBP) into one of two positions that will selectively destabilize the Y-fold and not the G-fold or *vice versa*. These sites are the turn between β10 and β11 in the Y-fold (site A in Figure 1B) or the turn between β9 and β10 in the G-fold (site B in Figure 1B), respectively. On binding FK506 or rapamycin, folding of the cpFKBP domain removes the entropic penalty and stabilizes the fold in which it is resident. We denote this switching mechanism as entropy switching AFF (esAFF).

Characterization of Sensor Components. We first purified and characterized the individual proteins from which the FP scaffold was assembled: the isolated CPs corresponding to the Y-fold (cpY) and G-fold (cpG) without any insertions into site A or B (Figure 1C, inset). We later define the Y-fold analogue and the G-fold analogue as cpY and cpG with insertions at site A and site B, respectively, as shown in Figure 1B. Cartoon representations of the sensors and analogues are shown in Figure 1D. Spectral characterization of cpG and cpY confirmed that their absorbance maxima (492 and 514 nm; Figure S1A) and emission maxima (509 and 524 nm; Figure 1C) remained unchanged from those of the parent FPs. As anticipated from previous studies,[21] Y203 increased the brightness of the chromophore: emission of cpY was 1.675-fold greater than that of cpG when both proteins were excited at 492 nm, as determined by integrating the areas under the curves (AUC) from 500 to 600 nm for each emission spectrum (Figure 1C). Guanidinium hydrochloride (GdmCl) denaturation experiments revealed that cpY is more stable than cpG, as judged by the apparent change in the Gibbs free energy of folding ($\Delta\Delta G_{fold}$ = 2.78 kcal/mol) and by the change in the midpoint of denaturation (ΔC_m = 0.80 M GdmCl) (Figure S1C and Table S1). The criteria for the target recognition domain in the esAFF design are that it: (i) has a short N−C terminal distance (less than or equal to the C_α−C_α distance between the residues at the ends of the loop into which it is inserted); (ii) is predominantly unfolded in the absence of a ligand; and (iii) folds on ligand binding. To shorten the 26 Å N−C length of WT FKBP, we circularly permuted it at position 33. Conveniently, cpFKBP is ∼50% unfolded without the ligand and fully folds upon binding FK506 or rapamycin (Figure S2A). Binding and folding occur within the dead time of mixing (∼10 s) (Figure S2B).

To create the esAFF biosensor, cpFKBP can either be inserted into the Y-fold or the G-fold (site A or site B; Figure 1B). We chose to insert cpFKBP into cpY (creating the Y-fold analogue) because cpY is more stable than cpG. Binding of FK506 to the Y-fold analogue had no effect on its fluorescence (Figure S1B). As expected, insertion of cpFKBP destabilized cpY, as evidenced by the lower C_m value of the Y-fold analogue (ΔC_m = 1.83 M GdmCl) (Figure S1C and Table S1). This finding lends support to the loop-closure entropy model. We could not, however, quantify this effect because the cooperativity parameter (m value) significantly increased (∼twofold) after cpFKBP insertion (Table S1). We also note that inserting a single Gly into site B of cpG (to create the G-fold analogue described below) also increased the apparent cooperativity of cpG unfolding to a similar extent (Figure S4). These large changes in m value suggest that insertion into these loops may reduce the population of an intermediate in the unfolding transition or allow unfolding/refolding to reach equilibrium more fully within the 24 h incubation time. GFP can take weeks to equilibrate, during which time C_m decreases steadily and m value fluctuates in a complex manner.[24] Either scenario complicates the interpretation of $\Delta\Delta G_{fold}$. Likewise, we were unable to measure the extent to which FK506 binding/cpFKBP folding stabilized the Y-fold analogue because the cpFKBP/FK506 complex unfolds at lower [GdmCl] compared to the Y-fold analogue.

***In Vitro* Sensor Performance.** To quantify the color changes, we unmixed the sensor emission spectra into linear combinations of green and yellow reference spectra (obtained from Figure 1C; see Experimental Section). The experimental spectra were reproduced adequately by the sum of the unmixed green and yellow AUCs (AUC_{green} and AUC_{yellow}), with no other fluorescent species detected (representative examples are shown in Figure S3). The yellow-to-green fluorescence ratio (Y/G) was defined as AUC_{yellow}/AUC_{green}, with $(Y/G)_{ON}$ and $(Y/G)_{OFF}$ corresponding to the values with the ligand or DMSO vehicle, respectively. The turn-on ratio—the main measure of sensor performance—was then calculated by dividing $(Y/G)_{ON}$ by $(Y/G)_{OFF}$.

https://doi.org/10.1021/acssensors.1c02239
ACS Sens. 2022, 7, 263−271

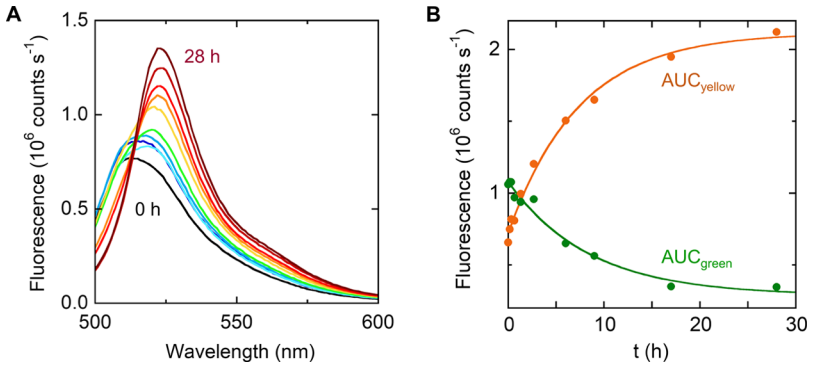

Figure 2. Sensor 2 is a ratiometric, ligand-induced color switch *in vitro*. (A) Unprocessed fluorescence spectra show a time-dependent shift from green to yellow emission after the addition of 20 μM FK506 (45 °C). Spectra were collected at time intervals between t = 0 (black) and t = 28 h (red). (B) Ratiometric response is quantified by unmixing the spectra in panel (A) into AUC_{yellow} (orange) and AUC_{green} (green) components. Fitting these data to a single exponential function (lines) reveal $t_{1/2} \sim 5$ h.

We also considered the possibility that the fluorescence change could be due in part to an AFF-independent mechanism, for example, ligand binding changing the protonation state of the mature chromophore or causing the chromophore to mature. Whether such processes contribute to the observed turn-on can be determined by comparing the increase in the concentration of Y-fold to the decrease in the concentration of G-fold, by adjusting the ratio of their AUC values with their difference in brightness (cpY was 1.675 times brighter than cpG when both were excited at 492 nm (Figure 1C); see Experimental Section). In other words, equal populations of Y-fold and G-fold would result in (Y/G) = 1.675, and if AUC_{yellow} increased by more than 1.675 times the value by which AUC_{green} decreased, then the excess amount would be attributed to additional chromophore formation in the Y-fold. For the *in vitro* experiments described below, we found that 90−110% of the observed color change could be explained by the AFF fold shift (Table 1), indicating that chromophore maturation/protonation did not contribute significantly to the switching mechanism *in vitro*.

Sensor 1 was constructed by inserting cpFKBP into site A of the FP scaffold, as shown in Figure 1B. We expected sensor 1 to express mostly in the G-fold because the G-fold analogue was more stable than the Y-fold analogue (Table S1). Surprisingly, the purified protein exhibited a (Y/G) value of 2.65, indicating that it expressed mostly in the Y-fold. We hypothesized that the Y-fold might be favored due to a kinetic folding trap, as proposed by Do and Boxer.[22] In their design as well as ours, the Y203-containing β10 strand is the first to emerge from the ribosome, and the T203-containing β10 strand is the last to exit. As the co-translational folding of GFP is efficient[25] and chromophore residues interact more favorably with Y203 than they do with T203,[22] it may potentially introduce a kinetic trap for the Y-fold. As a test, we unfolded sensor 1 with HCl (pH 2) and refolded by a rapid pH jump back to pH 7.5. Sensor 1 refolded mostly in the G-fold [(Y/G) = 0.13, Figure S3A], consistent with the kinetic trap hypothesis. Clark and co-workers reached a similar conclusion when they compared in-cell and *in vitro* folding of a chimeric FP consisting of an N-terminal domain (specifying yellow fluorescence) and a C-terminal domain (specifying blue fluorescence) that compete for folding with a shared central domain.[26] They attributed the twofold higher ratio of yellow-to-blue fluorescence in cells to a co-translational folding trap, which was exacerbated by substituting rare codons into the C-terminal domain gene. We applied the above unfolding/refolding procedure before testing all sensors *in vitro*.

Addition of FK506 to sensor 1 failed to produce a significant turn-on (Figure S3B). The likely reason is that the thermodynamic balance between the G-fold and the Y-fold is too far in favor of the former to be overcome by the loop-closure entropy gains to the latter. To bring them into a closer balance, we sought to selectively destabilize the G-fold using the same loop entropy strategy. We created G-fold analogues with 1-mer (Gly), 5-mer (GSGSG), and 10-mer (GGSGTSGGSG) unstructured peptides inserted into site B (Figure 1B). As with cpFKBP inserted into site A of cpY, all three peptide insertions increased the m value of GdmCl melts, rendering the interpretation of $\Delta\Delta G_{fold}$ unreliable. The single Gly insertion was sufficiently destabilizing, making the C_m and m values of the resulting G-fold analogue approximately equal to those of the Y-fold analogue (Figure S4). Increasing the insertion length to 5 and 10 residues produced only minor additional decreases in stability (Figure S4). We therefore constructed sensor 2 by inserting a single Gly into site B (Figure 1B). As expected, destabilizing the G-fold increased the (Y/G) value of the purified protein to 24 and that of the refolded protein to 0.86 ± 0.02 (Figure S5), the latter value being consistent with the near-equivalent stabilities of the G- and Y-folds.

We evaluated the performance of sensor 2 at 22, 37, and 45 °C. Visual inspection of the sensor 2 emission spectra confirmed a robust shift from green to yellow fluorescence upon FK506 addition at 45 °C (Figure 2A). The time-dependent spectral change resembled that of the theoretical shift from OFF to ON states, as visualized by the superposition of the isolated cpY and cpG spectra (Figure 1C). Unmixing the sensor 2 emission spectra revealed a (5.97 ± 0.83)-fold turn-on after FK506 exposure, relative to the DMSO vehicle control (Table 1). To measure the rate of the conformational shift in the presence of the ligand, we fit the time-dependent changes in AUC_{green} and AUC_{yellow} to single exponential functions (Figure 3B). Both half-times ($t_{1/2}$) were approximately equal at ~5 h (Table 1). The switching rates appeared to slow down with temperature, to the point where little change was observed at 22 °C or 37 °C over the course of 20 h (Table S2). To determine reversibility, we incubated sensor 2 with 15 μM FK506 for 9 h (Figure S7A) and then added 30 μM WT FKBP. No significant change in Y/G ratios was observed after

https://doi.org/10.1021/acssensors.1c02239
ACS Sens. 2022, 7, 263−271

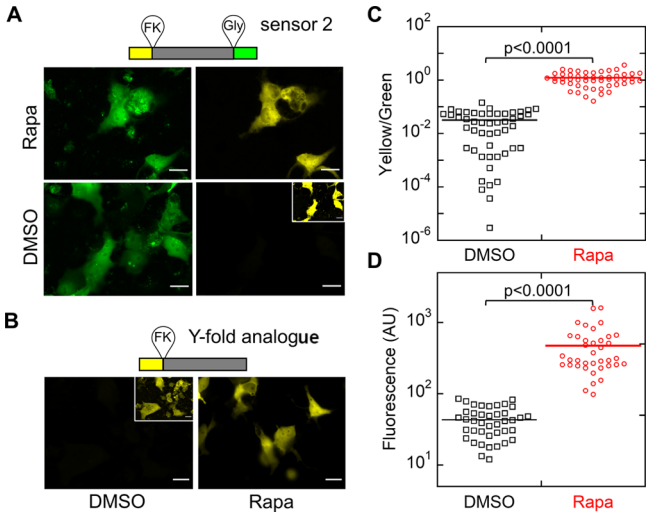

Figure 3. Sensor 2 and its Y-fold analogue show a large, intensiometric response in mammalian cells. (A) Representative fluorescence images are shown of COS-7 cells expressing sensor 2 and treated with 5 μM rapamycin (top) or DMSO vehicle (bottom) for 4 h. Images were acquired in green and yellow channels, and the relative contribution of G-fold and Y-fold was determined by unmixing the channels, as described in Experimental Section. Inset: the same image at higher contrast shows yellow fluorescence in cells treated with vehicle only, revealing that sensor 2 was expressed but only weakly fluorescent. (B) Representative images are shown of COS-7 cells expressing Y-fold analogue and treated with DMSO vehicle alone (left) or rapamycin (right). Inset: the same image in higher contrast shows that the Y-fold analogue is expressed in cells but is only weakly fluorescent without rapamycin. (C) Sensor 2 turn-on was quantified by dividing the integrated cell intensity in yellow channel by the integrated cell intensity in the green channel. Each point represents a cell. Data are representative of three biological repeats, as described in Experimental Section (DMSO, n = 49; rapamycin, n = 51). Data for the individual components of sensor 2 are shown in Figure S8. (D) Y-fold analogue turn-on was quantified by integrating the yellow fluorescence of cells expressing mKate2. Each dot represents a cell (DMSO, n = 38; rapamycin, n = 41). For panels (C,D), significance was determined by performing a two-tailed Student's t test with unequal variance. Scale bars are 10 μm.

40 h, indicating that the conformational change was irreversible on this timescale (Figure S7B).

To test whether oligomerization of sensor 2, perhaps mediated by domain swap, played a role in the observed color change, we performed size exclusion chromatography on sensor 2 that had been unfolded and refolded at 20 μM and treated with FK506 or DMSO vehicle. Chromatograms of the unfolded/refolded proteins were similar to that of the freshly purified sample (Figure S5). All three consisted of a monomeric peak at 15.6 mL and a small peak in the void volume. No additional, larger MW peaks appeared after FK506 addition. These data reveal that neither unfolding/refolding nor the subsequent addition of ligand induced oligomerization or aggregation, even at 20 μM sensor 2 (~100-fold greater than the concentration used in fluorescence switching experiments).

Test of the Entropy Switch Mechanism. The loop-closure entropy model holds that the Y-fold will be increasingly destabilized as the cpFKBP domain becomes more unstructured and flexible. To test this prediction, we unfolded and refolded sensor 2 as described above (45 °C), with the inclusion of GdmCl in the refolding buffer to unfold any structure that remained in the cpFKBP domain. We chose concentrations of GdmCl (0.15 and 0.3 M) that were sufficient to unfold free cpFKBP (Figure S2A) but too low to denature the cpFKBP−FK506 complex (Figure S2B), the Y-fold analogue, or the G-fold analogue (Figure S1B). $(Y/G)_{OFF}$ values decreased slightly from 0 to 0.15 M GdmCl. This trend indicates that 0.15 M GdmCl destabilized the Y-fold relative to the G-fold, consistent with GdmCl unfolding the residual structure in the cpFKBP domain. No further change in $(Y/G)_{OFF}$ was observed with 0.3 M GdmCl, suggesting that cpFKBP was fully unfolded by 0.15 M GdmCl. Sensor 2 turn-on ratios and rates in 0.15 and 0.3 M GdmCl were similar to the values without the denaturant (Table 1).

In further support of the loop-closure entropy model, $(Y/G)_{OFF}$ of sensor 2 progressively increased with the decreasing temperature of refolding (45, 37, and 22 °C; Figure S5D−F). This trend is likely caused by the cpFKBP domain folding at lower temperatures and thus stabilizing the Y-fold. Together, these data provide evidence for the esAFF mechanism *in vitro*.

Sensor Performance in Cells. To test if our genetically encoded biosensor functioned in mammalian cells, we transfected a gene encoding sensor 2 along with a N-terminal maltose-binding protein (MBP) tag into COS-7 cells and treated the cells with rapamycin or DMSO vehicle. The sensor 2 gene was co-transfected with the gene encoding for the red FP mKate2, and cells exhibiting red fluorescence were randomly selected for imaging in green and yellow channels. Cells were maintained at 37 °C throughout the experiments until they were imaged (<10 min at room temperature). We observed an 18-fold turn-on over DMSO vehicle alone within 30 min of adding rapamycin, with an average turn-on of (35 ± 9)-fold within 4 h over three biological repeats (Figure 3A). The turn-on half-time was (60 ± 10) min (Figure S8A). Sensor 2 responded to rapamycin in the expected dose-dependent manner (Figure S8B). Thus, sensor 2 performed exceedingly well in cells, achieving both a faster and a higher turn-on than that what was attained *in vitro*.

Two observations, however, indicate that the turn-on mechanisms were different in cells and *in vitro*. Turn-on *in vitro* could largely be accounted for by the conversion of G-fold to Y-fold *via* AFF-mediated conformational switching. By contrast, green fluorescence in transfected cells did not change significantly on rapamycin treatment (1.24 ± 0.53-fold). The change in (Y/G) was due almost exclusively to a large increase in yellow fluorescence (42 ± 23-fold), that is, a dark-to-yellow process (Figures 3A and S9). The second observation is that turn-on half-times were faster in cells (60 min at 37 °C) than *in vitro* (>4 h at 45 °C and significantly longer at 37 °C). These two findings suggest that turn-on arises from chromophore formation in the Y-fold in cells and from the slower AFF-mediated conformational change *in vitro* (see Discussion).

We propose that the different sensing mechanisms *in vitro* and in cells originate from the putative kinetic trap that exists when the sensors fold in cells, together with the difference in protein expression temperatures, as follows. Protein samples for *in vitro* experiments were expressed at 18 °C in *E. coli*. At this temperature, sensor 2 expresses as a bright yellow protein because it is trapped in the Y-fold, and folding as well as chromophore maturation are relatively efficient at low temperature. Unfolding and refolding *in vitro* bypass the kinetic trap, populating the G-fold and allowing the green-to-yellow fold shift to be observed. Sensor 2 was expressed in

https://doi.org/10.1021/acssensors.1c02239
ACS Sens. 2022, 7, 263−271

COS-7 cells at 37 °C, where it mostly adopts a third, dark conformation that becomes bright yellow after rapamycin exposure. Thus, the dark state is distinct from the Y-fold and the G-fold and appears to be closer in structure to the Y-fold.

There are two simple views of the dark state structure. First, the chromophore is mature but quenched, suggesting that the dark state resembles the native Y-fold but contains a defect that allows solvent access and protonation of the chromophore. Alternately, the chromophore may not be mature, implying that the dark state is more substantially misfolded such that it cannot provide the proper environment for cyclization. In either case, the dark state of sensor 2 appears to be a Y-fold-like conformation in which the Y-fold is partially folded/misfolded but stable and kinetically trapped, as opposed to being inherently unstable or able to unfold quickly. If the latter conditions were true, sensor 2 would readily adopt the G-fold when expressed in COS-7 cells.

The observed dark-to-yellow turn-on in COS-7 cells is best explained by the chromophore maturation model. The half-time of 60 min is consistent with chromophore cyclization, not with deprotonation of the mature chromophore, which is expected to occur quickly. In addition, when we purified sensor 2 from *E. coli* grown at 37 °C, we only observed a small absorbance peak from the native G-fold chromophore (492 nm; Figure S10) and not a peak indicative of a protonated or solvent-exposed Gly−Tyr−Gly chromophore (~400 nm).[27] If this view is correct, a likely reason why sensor 2 matures at 18 °C and not at 37 °C is that the cpFKBP domain is more disordered at the higher temperature. Lower temperatures (as well as FK506/rapamycin binding) stabilize cpFKBP, possibly tightening the Y-fold structure and facilitating chromophore maturation.

To test the hypothesis that sensor 2 turn-on in cells is due to the above mechanism and not the AFF-mediated fold shift, we transfected the Y-fold analogue gene into COS-7 cells and observed whether removing the second copy of β10 changed the magnitude or rate of the yellow fluorescence increase. The Y-fold analogue gene was also co-transfected with the mKate2 gene, and red fluorescent cells were randomly selected for imaging. As the Y-fold analogue has no green fluorescence, we calculated turn-on by the ratio of yellow intensities of rapamycin-treated *versus* vehicle-treated cells. The Y-fold analogue exhibited turn-on ((17 ± 7)-fold; Figure 3B) and $t_{1/2}$ (~50 min; Figure S8A) comparable to sensor 2, consistent with the chromophore maturation model. As a further test, we attempted to recapitulate the COS-7 results in *E. coli* by expressing sensor 2 and the Y-fold analogue at 37 °C. As expected, cell lysates exhibited only very weak yellow fluorescence (Figure S11). Addition of FK506 caused the yellow fluorescence to increase over several hours in the cell lysates, although not to the extent that was observed in COS-7 cells. No such increase was apparent when FK506 was added to the protein expressed at 18 °C (Figure S1B). These findings argue that the turn-on of sensor 2 (and the Y-fold analogue) at 37 °C is primarily driven by ligand-assisted cpFKBP folding and subsequent chromophore maturation in the Y-fold.

DISCUSSION

We have demonstrated that inserting a binding domain into an engineered FP scaffold results in a ligand-driven, color-changing biosensor that operates according to the AFF mechanism *in vitro*. Several principles emerge as being important to the design of this class of switches. First, the thermodynamic stabilities of the two folds must be made comparable. In the current design, the β10−β11 and β9−β10 loops in GFP are amenable to inserting a ligand-binding domain and a disordered peptide for tuning the relative stabilities of the Y-fold and G-fold, respectively, without severe loss of fluorescence. The second consideration is to employ a receptor domain with an N−C distance that is compatible with the ~9 Å distance between the C-terminus of β10 (S208) and the N-terminus of β11 (H217). There is likely some latitude in this distance requirement because we inserted the receptor between residues E213 and K214 in the eight-amino acid loop that connects β10 and β11, and the residues to either side may act as somewhat flexible linkers. Many proteins naturally possess short (≤5 Å) N−C lengths,[28] and for those that do not, circular permutation brings their new termini into proximity. Permutation sites can be identified using rational[29] or computational approaches.[30] Permutation typically destabilizes a protein, and if necessary, further destabilization can be achieved by permuting using short linkers to pinch the original termini together,[31] by introducing known mutations, or by chemical denaturants (Figure S6) and/or elevated temperature (Table S2).

Our study highlights how sensor behavior can change when it is expressed in cells *versus* refolded *in vitro*. The turn-on mechanism pivoted from an AFF-mediated green-to-yellow conformational change when sensor 2 was refolded to dark-to-yellow chromophore maturation when it was expressed in mammalian cells. Although the structural features of the chromophore microenvironment and molecular details remain unclear, this finding emphasizes the roles that protein translation and temperature may play in the folding and maturation of FPs. Of note, Do and Boxer reported that unfolding and refolding their related sensors also changed the relative populations of the two folds.[22]

Our AFF design blends elements of two main FP-based sensing mechanisms—bimolecular fluorescence complementation (BiFC) and that of single FP-based biosensors—and offers the potential of increased modularity. In BiFC sensors, the FP is bisected into two complementary, nonfluorescent fragments that are attached to proteins that dimerize in response to the ligand. An example is an N-terminal FP fragment fused to FKBP and the C-terminal FP fragment fused to FKBP-rapamycin-binding protein (FRB).[32] FKBP and FRB form a sandwich-type interaction with rapamycin. Dimerization increases the local concentration of the FP fragments, resulting in complementation and a turn-on that shares the same characteristics as that of sensor 2 and the Y-fold analogue (i.e., dark-to-fluorescent and typically irreversible). BiFC sensors are straightforward in their construction but are not especially modular because the recognition domain consists of two heterologous proteins that must associate only in the presence of a ligand. Finding natural protein partners that respond to a ligand of choice, or engineering proteins to do so, is often challenging. Additionally, the natural affinity that FP fragments have for one another makes turn-on dependent on sensor concentration, with spontaneous association and background fluorescence potential concerns.

Single FP-based biosensors can consist of a recognition domain inserted into the FP, as in the GCaMP family of calcium sensors,[33] or the FP fused to the recognition domain.[7,34] Both designs require that the recognition domain possess an inherent conformational change in response to binding. Perhaps, the simplest example of the latter class is a

https://doi.org/10.1021/acssensors.1c02239
ACS Sens. 2022, 7, 263−271

binding domain that undergoes an open-to-closed motion upon ligand binding, which is then detected by FRET between two well-placed FPs. GCaMPs are noteworthy because, like sensor 2, they typically produce a dark-to-bright output in cells. In GCaMPs, the calmodulin (CaM) receptor domain and the M13/RS20 peptide are fused to an FP, at a point that abuts the chromophore.[35] Binding of Ca^{2+} to CaM causes it to associate with M13. This conformational change is transmitted to the FP, altering the local chemical environment around the chromophore and increasing its brightness. Sensor 2 behaves differently from GCaMPs in three respects. First, GCaMP chromophores mature in cells in the absence of a ligand. Turn-on is consequently much faster than that of sensor 2 or the Y-fold analogue, and it is readily reversible. The second distinction is that GCaMP sensors are typically monochromatic, and their output is consequently intensity only. The readout of sensor 2 is intensiometric in cells but is ratiometric when the sensor is unfolded and refolded *in vitro*. The last difference is that GCaMPs, like BiFC sensors, require a specialized receptor domain that binds to a partner in the presence of the target analyte.

The AFF design employs two principles—binding-induced folding and loop-closure entropy—that are more readily implemented into the existing binding domains that do not possess natural conformational change mechanisms. Any protein can be destabilized to the point of unfolding (e.g., by mutation or truncation), and binding and folding are naturally coupled processes. The N−C terminal distance of any protein can be made to be nearly zero (by circular permutation) and can be widened as needed (by adding linker residues), thus enabling insertion into surface loops and turns of a host protein with minimal structural perturbation of either protein. Aggregation and proteolytic degradation, however, remain potential concerns when making these modifications.

The main limitations with sensor 2 are the slow rate of the AFF-mediated fold shift and that ratiometric output requires prior unfolding and refolding. Both phenomena are likely manifestations of local energy minima deepened by GFP's high thermodynamic stability and slow unfolding. For example, exchange of β10 strands requires breaking of numerous H bonds to the adjacent strands and disruption of hydrophobic packing interactions. Our switch design may be improved in the future by introducing packing mutations in β10 or of residues in contact with β10, to weaken its affinity for the β-barrel. This would likely enable switching to be reversible as well.

Nevertheless, sensor 2's 35-fold intensiometric turn-on in cells and sixfold ratiometric response *in vitro* match those of other single FP-based genetically encoded fluorescent sensors for Ca^{2+},[36] glucose,[7] citrate,[37] and the GECO[38] and GCaMP designs.[39] Due to the large fold-change and irreversible nature of their fluorescence turn-on, we envision that esAFF sensors (and their Y-fold analogues) may find utility in cellular applications in which one desires to detect targets that are present at very low concentrations, where signal accumulation is advantageous.

A question that remains to be addressed is whether this design strategy can be applied to detect a range of useful biological targets in cells. In addition to its application in cellular sensing, the findings from this study can expand the protein engineers' toolbox as it provides insights into how to create custom input and output functions by using a combination of protein engineering techniques: AFF of the output domain and circular permutation of the input domain. These characteristics confer modularity and may aid in the development of broadly applicable engineered protein switches.[40]

■ ASSOCIATED CONTENT

Supporting Information

The Supporting Information is available free of charge at https://pubs.acs.org/doi/10.1021/acssensors.1c02239.

Biophysical characterization of protein constructs used in the study (G-fold analogues, Y-fold analogues, cpFKBP, and sensor 2); fluorescence images and analysis of COS-7 cells transfected with sensor 2 and Y-fold analogue genes; amino acid sequences of all protein constructs; thermodynamic parameters; and yellow-green turn-on ratios of protein constructs (PDF)

■ AUTHOR INFORMATION

Corresponding Author

Stewart N. Loh − *Department of Biochemistry and Molecular Biology, SUNY Upstate Medical University, Syracuse, New York 13210, United States;* orcid.org/0000-0003-4387-9644; Email: lohs@upstate.edu

Authors

Anna Miriam John − *Department of Biochemistry and Molecular Biology, SUNY Upstate Medical University, Syracuse, New York 13210, United States*

Harsimranjit Sekhon − *Department of Biochemistry and Molecular Biology, SUNY Upstate Medical University, Syracuse, New York 13210, United States*

Jeung-Hoi Ha − *Department of Biochemistry and Molecular Biology, SUNY Upstate Medical University, Syracuse, New York 13210, United States*

Complete contact information is available at: https://pubs.acs.org/10.1021/acssensors.1c02239

Author Contributions

A.M.J. and H.S. contributed equally. The manuscript was written through contributions of all authors. All authors have given approval to the final version of the manuscript.

Funding

This work was supported by NIH grant R01GM115762 to S.N.L.

Notes

The authors declare no competing financial interest.

■ ABBREVIATIONS

FP, fluorescent protein; CP, circular permutant; esAFF, entropy-switching alternate frame folding; GdmCl, guanidinium chloride; BiFC, bimolecular fluorescence complementation

■ REFERENCES

(1) Adamson, H.; Jeuken, L. J. C. Engineering Protein Switches for Rapid Diagnostic Tests. *ACS Sens.* **2020**, *5*, 3001−3012.

(2) Gräwe, A.; Stein, V. Linker Engineering in the Context of Synthetic Protein Switches and Sensors. *Trends Biotechnol.* **2021**, *39*, 731−744.

(3) Stein, V.; Alexandrov, K. Synthetic Protein Switches: Design Principles and Applications. *Trends Biotechnol.* **2015**, *33*, 101−110.

(4) Stratton, M. M.; Loh, S. N. Converting a Protein into a Switch for Biosensing and Functional Regulation. *Protein Sci.* **2011**, *20*, 19−29.
(5) Lane, M. D.; Seelig, B. Advances in the Directed Evolution of Proteins. *Curr. Opin. Chem. Biol.* **2014**, *22*, 129−136.
(6) Shui, S.; Gainza, P.; Scheller, L.; Yang, C.; Kurumida, Y.; Rosset, S.; Georgeon, S.; Di Roberto, R. B.; Castellanos-Rueda, R.; Reddy, S. T.; Correia, B. E. A Rational Blueprint for the Design of Chemically-Controlled Protein Switches. *Nat. Commun.* **2021**, *12*, 5754.
(7) Nadler, D. C.; Morgan, S.-A.; Flamholz, A.; Kortright, K. E.; Savage, D. F. Rapid Construction of Metabolite Biosensors Using Domain-Insertion Profiling. *Nat. Commun.* **2016**, *7*, 12266.
(8) Langan, R. A.; Boyken, S. E.; Ng, A. H.; Samson, J. A.; Dods, G.; Westbrook, A. M.; Nguyen, T. H.; Lajoie, M. J.; Chen, Z.; Berger, S.; Mulligan, V. K.; Dueber, J. E.; Novak, W. R. P.; El-Samad, H.; Baker, D. De Novo Design of Bioactive Protein Switches. *Nature* **2019**, *572*, 205−210.
(9) Alberstein, R. G.; Guo, A. B.; Kortemme, T. Design Principles of Protein Switches. *Curr. Opin. Struct. Biol.* **2022**, *72*, 71−78.
(10) Tainaka, K.; Sakaguchi, R.; Hayashi, H.; Nakano, S.; Liew, F. F.; Morii, T. Design Strategies of Fluorescent Biosensors Based on Biological Macromolecular Receptors. *Sensors* **2010**, *10*, 1355−1376.
(11) Scalley-Kim, M. Low Free Energy Cost of Very Long Loop Insertions in Proteins. *Protein Sci.* **2003**, *12*, 197−206.
(12) Stratton, M. M.; Mitrea, D. M.; Loh, S. N. A Ca^{2+}-Sensing Molecular Switch Based on Alternate Frame Protein Folding. *ACS Chem. Biol.* **2008**, *3*, 723−732.
(13) Stratton, M. M.; Loh, S. N. On the Mechanism of Protein Fold-Switching by a Molecular Sensor. *Proteins* **2010**, *78*, 3260−3269.
(14) Ha, J.-H.; Shinsky, S. A.; Loh, S. N. Stepwise Conversion of a Binding Protein to a Fluorescent Switch: Application to Thermoanaerobacter Tengcongensis Ribose Binding Protein. *Biochemistry* **2013**, *52*, 600−612.
(15) Ha, J.-H.; Tu, H.-C.; Wilkens, S.; Loh, S. N. Loss of Bound Zinc Facilitates Amyloid Fibril Formation of Leukocyte-Cell-Derived Chemotaxin 2 (LECT2). *J. Biol. Chem.* **2021**, *296*, 100446.
(16) Bolen, D. W.; Santoro, M. M. Unfolding Free Energy Changes Determined by the Linear Extrapolation Method. 2. Incorporation of Delta G Degrees N-U Values in a Thermodynamic Cycle. *Biochemistry* **1988**, *27*, 8069−8074.
(17) Jordan, M.; Schallhorn, A.; Wurm, F. M. Transfecting Mammalian Cells: Optimization of Critical Parameters Affecting Calcium-Phosphate Precipitate Formation. *Nucleic Acids Res.* **1996**, *24*, 596−601.
(18) Schindelin, J.; Arganda-Carreras, I.; Frise, E.; Kaynig, V.; Longair, M.; Pietzsch, T.; Preibisch, S.; Rueden, C.; Saalfeld, S.; Schmid, B.; Tinevez, J.-Y.; White, D. J.; Hartenstein, V.; Eliceiri, K.; Tomancak, P.; Cardona, A. Fiji: An Open-Source Platform for Biological-Image Analysis. *Nat. Methods* **2012**, *9*, 676−682.
(19) Lam, A. J.; St-Pierre, F.; Gong, Y.; Marshall, J. D.; Cranfill, P. J.; Baird, M. A.; McKeown, M. R.; Wiedenmann, J.; Davidson, M. W.; Schnitzer, M. J.; Tsien, R. Y.; Lin, M. Z. Improving FRET Dynamic Range with Bright Green and Red Fluorescent Proteins. *Nat. Methods* **2012**, *9*, 1005−1012.
(20) Weber, W.; Helms, V.; McCammon, J. A.; Langhoff, P. W. Shedding Light on the Dark and Weakly Fluorescent States of Green Fluorescent Proteins. *Proc. Natl. Acad. Sci. U. S. A.* **1999**, *96*, 6177−6182.
(21) Jung, G.; Wiehler, J.; Zumbusch, A. The Photophysics of Green Fluorescent Protein: Influence of the Key Amino Acids at Positions 65, 203, and 222. *Biophys. J.* **2005**, *88*, 1932−1947.
(22) Do, K.; Boxer, S. G. GFP Variants with Alternative β-Strands and Application as a Light-Driven Protease Sensor: A Tale of Two Tails. *J. Am. Chem. Soc.* **2013**, *135*, 10226−10229.
(23) Minard, P.; Scalley-Kim, M.; Watters, A.; Baker, D. A "loop Entropy Reduction" Phage-Display Selection for Folded Amino Acid Sequences. *Protein Sci.* **2001**, *10*, 129−134.
(24) Huang, J.-r.; Craggs, T. D.; Christodoulou, J.; Jackson, S. E. Stable Intermediate States and High Energy Barriers in the Unfolding of GFP. *J. Mol. Biol.* **2007**, *370*, 356−371.
(25) Ugrinov, K. G.; Clark, P. L. Cotranslational Folding Increases GFP Folding Yield. *Biophys. J.* **2010**, *98*, 1312−1320.
(26) Sander, I. M.; Chaney, J. L.; Clark, P. L. Expanding Anfinsen's Principle: Contributions of Synonymous Codon Selection to Rational Protein Design. *J. Am. Chem. Soc.* **2014**, *136*, 858−861.
(27) Nagai, T.; Sawano, A.; Park, E. S.; Miyawaki, A. Circularly Permuted Green Fluorescent Proteins Engineered to Sense Ca^{2+}. *Proc. Natl. Acad. Sci. U.S.A.* **2001**, *98*, 3197−3202.
(28) Krishna, M. M. G.; Englander, S. W. The N-Terminal to C-Terminal Motif in Protein Folding and Function. *Proc. Natl. Acad. Sci. U. S. A.* **2005**, *102*, 1053−1058.
(29) Ha, J.-H.; Presti, M. F.; Loh, S. N. A Single Protein Disruption Site Results in Efficient Reassembly by Multiple Engineering Methods. *Biophys. J.* **2019**, *117*, 56−65.
(30) Dagliyan, O.; Krokhotin, A.; Ozkan-Dagliyan, I.; Deiters, A.; Der, C. J.; Hahn, K. M.; Dokholyan, N. V. Computational Design of Chemogenetic and Optogenetic Split Proteins. *Nat. Commun.* **2018**, *9*, 4042.
(31) Butler, J. S.; Mitrea, D. M.; Mitrousis, G.; Cingolani, G.; Loh, S. N. Structural and Thermodynamic Analysis of a Conformationally Strained Circular Permutant of Barnase. *Biochemistry* **2009**, *48*, 3497−3507.
(32) DeRose, R.; Miyamoto, T.; Inoue, T. Manipulating Signaling at Will: Chemically-Inducible Dimerization (CID) Techniques Resolve Problems in Cell Biology. *Pflügers Archiv* **2013**, *465*, 409−417.
(33) Nakai, J.; Ohkura, M.; Imoto, K. A High Signal-to-Noise Ca2+ Probe Composed of a Single Green Fluorescent Protein. *Nat. Biotechnol.* **2001**, *19*, 137−141.
(34) Nasu, Y.; Shen, Y.; Kramer, L.; Campbell, R. E. Structure- and Mechanism-Guided Design of Single Fluorescent Protein-Based Biosensors. *Nat. Chem. Biol.* **2021**, *17*, 509−518.
(35) Akerboom, J.; Rivera, J. D. V.; Guilbe, M. M. R.; Malavé, E. C. A.; Hernandez, H. H.; Tian, L.; Hires, S. A.; Marvin, J. S.; Looger, L. L.; Schreiter, E. R. Crystal Structures of the GCaMP Calcium Sensor Reveal the Mechanism of Fluorescence Signal Change and Aid Rational Design. *J. Biol. Chem.* **2009**, *284*, 6455−6464.
(36) Baird, G. S.; Zacharias, D. A.; Tsien, R. Y. Circular Permutation and Receptor Insertion within Green Fluorescent Proteins. *Proc. Natl. Acad. Sci. U.S.A.* **1999**, *96*, 11241−11246.
(37) Zhao, Y.; Shen, Y.; Wen, Y.; Campbell, R. E. High-Performance Intensiometric Direct- and Inverse-Response Genetically Encoded Biosensors for Citrate. *ACS Cent. Sci.* **2020**, *6*, 1441−1450.
(38) Zarowny, L.; Aggarwal, A.; Rutten, V. M. S.; Kolb, I.; Patel, R.; Huang, H.-Y.; Chang, Y.-F.; Phan, T.; Kanyo, R.; Ahrens, M. B.; Allison, W. T.; Podgorski, K.; Campbell, R. E. Bright and High-Performance Genetically Encoded Ca^{2+} Indicator Based on MNeon-Green Fluorescent Protein. *ACS Sens.* **2020**, *5*, 1959−1968.
(39) Qian, Y.; Rancic, V.; Wu, J.; Ballanyi, K.; Campbell, R. E. A Bioluminescent Ca^{2+} Indicator Based on a Topological Variant of GCaMP6s. *Chembiochem* **2019**, *20*, 516−520.
(40) John, A. M.; Sekhon, H.; Ha, J.-H.; Loh, S. N. Engineering a Fluorescent Protein Color Switch Using Entropy-Driven Beta Strand Exchange, **2021**. bioRxiv:10.20.465183.

https://doi.org/10.1021/acssensors.1c02239
ACS Sens. 2022, 7, 263−271